

Frequency Signal Source's PN (Phase Noise) Measurements: Challenges and Uncertainty

Ulrich L. Rohde
BTU Cottbus 03046 Germany

Ajay K. Poddar
Synergy Microwave NJ USA

Enrico Rubiola
FEMTO-ST Inst. Besancon France

Marius A. Silaghi
University of Oradea, Romania

Abstract—This paper describes oscillator noise measurement techniques, challenges and associated measurement uncertainty. The cross-correlation method used in modern PN measurement equipments, can present erroneous result, depending upon phase-inversion, harmonics, o/p load mismatch, and cable length. This discussion is imperative for low phase noise signal sources, validated with 2.4 GHz SAW oscillator, and discussed steps for mitigating these issues by using filtering/phase-matching N/W.

Keywords—Cross-Correlation, Oscillator, Phase Noise

I. INTRODUCTION

Prediction and estimation of oscillator phase noise is highly desirable for accurate timing, and other measuring purpose. Several noise models developed for estimating the phase noise dynamics of oscillator systems [1]-[6].

A. Oscillator Phase Noise Model

The simplest noise model is linear time invariant (LTIV) system in which oscillator's output considered as a resonant response to the input noise [1]-[2]. However, LTIV model fails to explain the uncertainty in the phase of noise upon each addition of noise to the autonomous oscillatory field) [7]. Consequently, relative phase between the signal and the added noise results in partition of the noise perturbation into quadrature of amplitude and phase, forming the basis for linear time variant (LTV) model [2]-[3]. The LTV model addresses the issues of LTIV approach by linearizing the oscillator phase, however introduces nonphysical artifact of infinite spectral power at frequencies approaching the carrier signal. The scientific alternative is nonlinear time variant (NLTV) model. NLTV techniques uses perturbation method based on numerical techniques, involves rigorous stochastic differential equations [4]-[6]. The NLTV approach applies Floquet theory to demonstrate the oscillator spectrum to be a Lorentzian for white-noise perturbation. The Lorentzian distribution [4] institutes the power at the oscillation frequency to be finite, mitigate the problems of infinite power [1, 3]. Although, the NLTV approach is precise, consequential solution is non-intuitive and not easy to apply since it requires comprehensive analysis of the oscillator dynamics, e.g., the determination of the time consuming Floquet eigenvectors [7].

Table 1 shows the comparative analysis of 3-most cited phase noise models (LTIV, LTV, and NLTV) [1]-[6]. One can argue the superiority of any of the three models based on easy to use, accuracy, reliability, simulation time, and convergence for a given oscillator topology. The ultimate goal of unified noise model is still a subject of discussion, what is needed to have an intuitive functional description of oscillator phase noise, comparable to the empirical model proposed by Leeson [1], but incorporates physics based technique [8].

Similarly, the reliable phase noise (PN) measurement is a difficult and time-consuming task. .

B. Phase Noise Measurement Challenges And Uncertainty

The PN measurement is ratiometric measurement, which requires high dynamic range to perform reliable measurement. The most effective methods therefore rely on removing carrier (by filtering or phase/frequency detection), so removing the reference value for any measurements. This may lead to "stitching" errors in the phase noise plots, which can be noticed when the PN measurement equipment changes settings to measure noise at different offset frequencies.

It is common to witness a test system produce a phase noise plot where the phase noise suddenly changes in level by a few dB's. It is typically a sign that the calibration of the plot is incorrect and the measured data cannot be relied. The problem frequently arises because the equipment changes bandwidth and other critical setting (amplifier or PLL setting) that has an impact on the correction values applied to the measurement. Sometimes it can indicate that part of the test system is overloaded during one set of measurements. These errors make it tricky to assign a traceability figure to phase noise measurements.

The software algorithm in the PN measurement equipment may attempt to categorize noise and spurious signals, and correct the reading automatically in real time. Unfortunately, software do not succeed all time, particularly when the signal is slightly above the surrounding noise levels. The software algorithm can be made efficient by narrowing measurement bandwidth (at the expense of measurement time), because this lowers the level of the measured noise compared to the spurious signal. This makes it easier for the software to distinguish between noise and a spurious signal for a given spurious signal level; this only moves the problem to a lower level but never eradicate the problems.

Table 1: Describes the strengths and weaknesses of the noise models

Model	Leeson [1]	Lee and Hajimiri [2,3]	Kaertner and Demir [4,5,6]
Assumptions	LTIV	LTV	NLTV
Perturbing noise Source	white noise (KTB)	Cyclostationary $1/f^k$ for any $k \in \mathbb{N}$	Modulated $1/f^k$ for any $k \in \mathbb{N}$
Accuracy	Reasonable	Good	Exact
Simplicity	Simple	Moderate	Involved
Computer dependence	Independent (Calculation by hand)	Computer to evaluate ISF	Computer dependent (no closed form sol.)
Predicts close-in PN	No	Yes	Yes
Retained circuit info parameters	Loaded Q-factor (Q_L), O/P power P_s	q_{max}	None

Besides the concern of identifying spurious signals and noise, instruments use subtle method to expand the displayed dynamic range or to make noise signals appear to be practical and reasonable. These artifacts can be problematic, may lead to error in interpreting the real signal levels measured. The manufacturer of commercially PN measurement instruments continuously putting effort to improve the measurement method, and consequently may be able to take measures that partially overcome but in most cases disguise the limitations.

C. Influence of Harmonics on Phase Noise Measurement

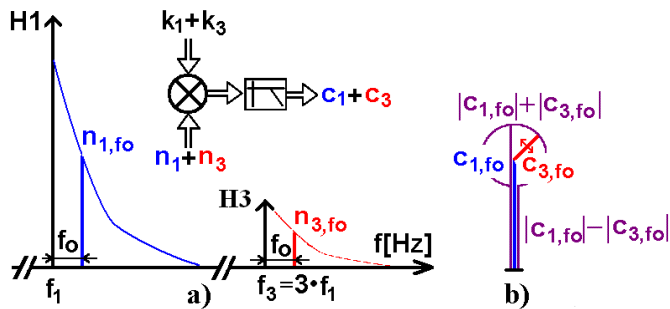
For low phase noise measurement, we noticed that third order harmonics and equipment dynamic ranges influence the measurement with greater degree. Device under test (DUT) harmonics can influence significantly on PN measurement accuracy. For validation, we postulate that the DUT's harmonics are combined by the mixers and contribute to phase noise measurement variations. The mixers convert to baseband the fundamental and the harmonics of the signal generated by the DUT. Because the noise components of the harmonics and the fundamental are correlated their combination depends on the phase delay between the harmonics.

Figure 1(a) shows the spectral components of the DUT signal. H1 and H3 are the fundamental and the 3rd harmonic, n_{1,f_0} and n_{3,f_0} are the phase noise (PN) associated with H1 and H3 at an offset frequency (f_0). The 3rd harmonic noise is correlated to the noise of the fundamental and its level is 9.542dBc higher. For ease, amplitudes of the fundamental and of the 3rd harmonic, H1 and H3, are not represented to scale.

In Figure 1(b), c_{1,f_0} and c_{3,f_0} represent PN associated with H1 and H3 that were down-converted. The PN associated with the 3rd harmonic and fundamental will be added as two rotating vectors. The magnitude of this component depends on the relative phase between the 3rd harmonic and fundamental. The resulting PN measurement uncertainty (peak-to-peak) at any given offset frequency is:

$$\frac{c_{f_0, \max}}{c_{f_0, \min}} [dB] = 20 \log \left(\frac{1 + 3 \frac{k_3 H_3}{k_1 H_1}}{1 - 3 \frac{k_3 H_3}{k_1 H_1}} \right) \quad (1)$$

The phase of the 3rd harmonic is rotated over 360 degrees producing a maximum and a minimum of the c_{f_0} signal.



f_1, f_3 - fundamental, 3rd harmonic frequency
 H_1, n_1, H_3, n_3 - Amplitude and Phase noise at f_1, f_3
 k_1, k_3 - mixer conversion loss at f_1, f_3
 c_1, c_3 - downconversion of n_1, n_3

Fig. 1: (a) Spectral components of DUT signal, and b) down-conversion products

Figure (2) illustrates the set-up, Signal Source Analyzer (SSA) used to measure phase noise of a signal, rich in harmonics. We use Rhode & Schwarz SPREF Reference Synthesizer, which can generate a 1GHz signal with 13dBm power, -35dBc harmonic content and a phase noise of -149 dBc at 10 kHz offset. The SPREF harmonically produces 2, 3, 4, 5, and 6GHz and these frequencies are available simultaneously on different outputs, all internally locked to a common crystal.

For the first part of the experiment, we selected the 1GHz and 3GHz outputs. The 3GHz output is passed through a variable attenuator and through a coaxial phase shifter (Narda's model 3752), then is added to the 1GHz reference by means of a 6dBc resistive divider. The 3GHz signal is produced harmonically from the 1GHz signal and thus their phases are coherent. The cables, variable attenuator and power combiner determine the relative position of the 3GHz with respect to 1GHz. With the help of phase shifter, the phase of 3GHz signal's can be rotated 360 degrees to perform the measurements. In Fig. 3 we present the results captured while using 6dB, 12dB and 19dB attenuator and rotating the phase of the 3GHz signal in 30 degrees increments from 0 to 360 degrees. We take the phase noise plot at 10 kHz offset and show the variation trend based on the phase shift delay. We plot the phase shift in radians while emphasizing that the origin is arbitrarily set by the cable length. The PN measured with the 3GHz signal not connected was -149.1dBc. With the 6dB attenuator, the amplitude of the signal at the phase noise analyzer is +6.2dBm for the 1GHz and -0.7dBm for the 3GHz. The corresponding 3rd harmonic levels, considering 1dB loss through the coaxial phase shifter, are -7, -13 and -20dBc. As we can see in Fig. 3, a 3rd harmonic with a level of -7dBc is showing a variation between -8 and +4dB around the level measured without harmonics. We can also observe that the values at 6.28 radians are approximately equal with the values at 0 radians as expected from a shift over 360 degrees.

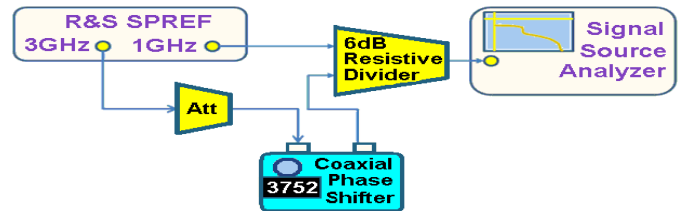


Fig. 2 Instrument setup for generating signals with harmonics and measuring the phase noise

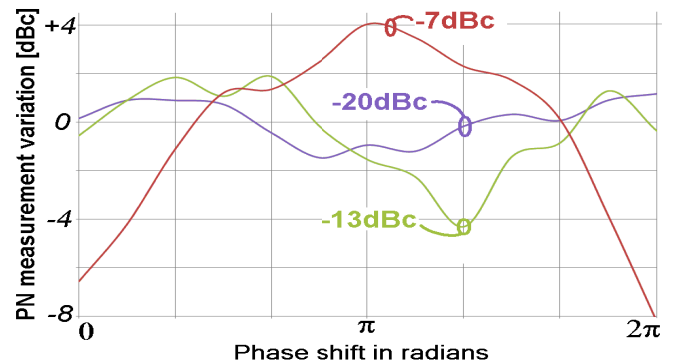


Fig. 3: PN depending on phase shift delay and harmonic level

With a harmonic level of -20dBc exhibits a variation of +1.1/-1.5dB. This suggests that using a filter that reduces the level of harmonics to below -20dBc would reduce the uncertainty to +/-1dB. We verified the 2nd, 4th and 5th harmonic contribution using the 2, 4 and 5GHz outputs from the SPREF. In summary, a -7dBc 2nd harmonic has shown a variation about +/-2dB, while the -13dBc results were in the range of +/-1dB. The 4th and 5th harmonics were showing no discernible variation of uncertainty of measurements over all phases. Figure (4) shows the relationship between phase noise and the conversion loss difference between the fundamental and third harmonic, for various levels of 3rd harmonic content in the signal presented at the input of the test equipment. The phase noise variations shown in Figure (4) are observed when fundamental is presented with high harmonic content at the input to the test equipment. These mixers (double balanced, image reject or triple balanced mixers) suppress the even order and as such show no significant variations in the case of even harmonics, while the 5th harmonic conversion loss is high enough and does not create measurement issues.

Analyzing Figure (4) if the mixer has a conversion loss difference between the fundamental and the 3rd harmonic of 7.5dB and the 3rd harmonic level is -7dBc (Red trace) we can expect a phase noise measurement variation of about 12dB (Red dot in Fig. 4, corresponding to the red trace in Fig. 3). For the same signal, if the conversion loss difference would be greater than 23dB, we could achieve a measurement variation smaller than +/-1dB. However, if the signal has a 3rd harmonic with a level of -20dBc (Green trace), and the conversion loss difference (between fundamental and 3rd) is higher than 10dB then the phase noise uncertainty will be less than +/- 1 dB.

All phase noise measurement methods that use mixers to down-convert the signal to baseband are subject to the effects described in Figure (4). The Phase Detector method and the Residual Phase Noise method will also demonstrate similar behavior. If the mixed signals have harmonics, the mechanism that converts the harmonics to baseband will degrade the measurement accuracy.

D. Estimation of Uncertainty

For reliable measurement, estimation of uncertainty is key requirement. As per guidelines [9], measurement uncertainty grouped into two categories: type-A (statistical), and type-B (various components-instruments and temperature control).

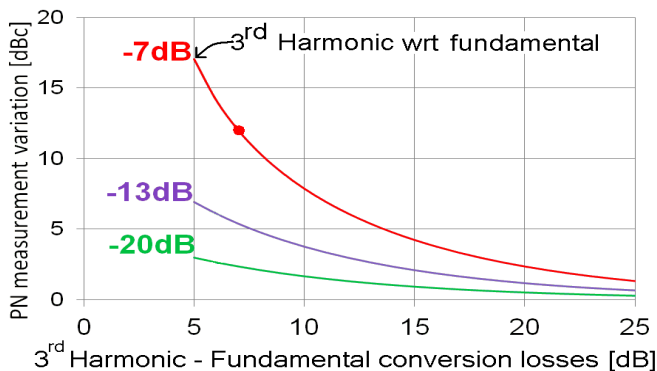


Fig. 4: Phase noise uncertainty estimate peak-to-peak (1) for different levels of 3rd harmonic with respect to fundamental.

The type “A” characterized by estimated variances, accounts for statistical methods such as reproducibility, repeatability, special consideration about Fast Fourier Transform analysis, and the experimental standard deviation. The type “B”, accounts for uncertainty due to instruments and temperature control variable; characterized by quantities that may be considered as approximations to the corresponding variances, the existence of which is assumed [10].

There are several methods to estimate the uncertainty and measure the PN of signal sources. However, it is essential to know the weaknesses-strengths of different measurement techniques, since none of these methods are correct for every situation. The modern cross-correlation engine takes into the account of most part of the uncertainty associated with the PN measurement instruments. Many test and measurement manufacturers implement cross-correlation techniques in one form or another to produce best phase noise measurement instruments available in the market today. However, cross-correlation engines is not flawless, simultaneous presence of correlated and anti-correlated signals can lead to gross underestimation of the total signal in cross-spectral analysis at localized offset or over a wide range of frequencies [11]-[12].

II. OSCILLATOR PHASE NOISE MEASUREMENT

The oscillator noise is normally described in terms of the power spectrum density $S(f)$ of the amplitude and phase noise, thus $S_a(f)$ and $S_\phi(f)$, as a function of the Fourier frequency f . Designers should be aware that the effect of amplitude noise may not be negligible, and that the resonant frequency of some resonators may be affected by the amplitude. The first definition of phase noise $\mathcal{L}(f)$ was given as $\mathcal{L}(f) = (\text{SSB power in 1Hz bandwidth})/(\text{carrier power})$. The problem with this definition is that it does not divide AM noise from PM noise, which yields to ambiguous results [11]. The IEEE Std 1139-1999 [13] redefines $\mathcal{L}(f)$ as $\mathcal{L}(f) = (1/2) \times S_\phi(f)$.

The physical unit of $S_\phi(f)$ is rad^2/Hz . Phase noise spectra are plotted on a log-log scale. $\mathcal{L}(f)$ is always given in dBc/Hz, which stands for dB below the carrier in 1-Hz bandwidth. In decibels, $\mathcal{L}(f) = S_\phi(f) - 3\text{dB}$. The fact that phase noise expressed in terms of the relative power (to the total carrier power) in a 1 Hz BW does not mean that the signal measured in a 1 Hz bandwidth. The phase noise data displayed by the equipment normalized to 1Hz measurement bandwidth. The modern phase noise measurement equipment measure the phase noise in measurement bandwidths, which increases with increasing carrier offset frequency. This is done for two reasons: (1) it results in shorter overall measurement time, and (2) at high carrier offset frequency (> 100 kHz), many measurement systems employ analog spectrum analyzers that are not capable of 1Hz resolution.

Noise measured in a 1 kHz bandwidth, for example, is 30dB higher than that displayed in a 1Hz bandwidth. That means that low-level discrete spurious signals (and narrowband noise peaks typically encountered under vibration due to high Q mechanical resonances) will go undetected. The second problem is that the commercial available software employed in the PN measurement equipment discriminates between random noise and discrete spurious signals but when

a reasonably sharp increase in noise level is detected; the system software assumes that the increase marks the presence of a “zero bandwidth” discrete signal. It is therefore when displaying the phase noise on a 1Hz bandwidth basis, applies a bandwidth correction factor to the random noise, but does not make a correction to what is interpreted as a discrete signal. This results in an erroneous plot if/when the detected “discrete” is really a narrowband noise peak.

A. Phase Noise Measurement Techniques

Following are the primary phase noise measurement techniques, listed in the order of increasing precision: (i) Direct Spectrum Technique, (ii) Frequency discriminator method–Heterodyne digital discriminator method, (iii) Phase detector techniques–Reference source/PLL method, (iv) Residual Method, and (v) 2-channel cross-correlation technique. The Direct Spectrum Method, PLL method, delay line discriminator method, and cross-correlation methods are frequently used to measure the oscillator phase noise. The first one is the simplest and has the biggest limitation. The last one requires the most complex measurement system but is the most versatile, can measure PN performance better than that of its reference oscillator.

Figure (5) shows the typical block diagram of the 2-channel cross-correlation technique. The oscillator under test is measured simultaneously by two separate phase-to-voltage transducers (in the dashed boxes), and by a dual-channel FFT analyzer. The O/P of each channel as shown in Figure (5) is

$$x(t) = a(t) + c(t) \leftrightarrow X(f) = A(f) + C(f) \quad (2)$$

$$y(t) = b(t) + c(t) \leftrightarrow Y(f) = B(f) + C(f) \quad (3)$$

where $a(t)$, $b(t)$ and $c(t)$ are random signals; $a(t)$ and $b(t)$ are the noise of the transducers, and $c(t)$ is the DUT noise; the upper case is used for the Fourier transform, and the ‘ \leftrightarrow ’ stands for the transform / inverse-transform pair. All signals are sampled at a suitable rate, and each acquisition takes the measurement time T . The PSD (Power Spectral Density) is a complex concept of mathematical probability, defined as the Fourier transform of the covariance function. The cross PSD is

$$S_{yx}^1(f) = \frac{2}{T} Y(f) X^*(f) \quad (4)$$

where the superscript ‘1’ means single-sided (no negative frequencies) and will be omitted hereinafter; the symbol ‘*’ means complex conjugate; and the factor ‘2’ is necessary for power consistency, after removing the negative frequencies.

Equation (4) implies the mathematical expectation, which in experiments is replaced with the average over a suitable number ‘ m ’ of samples, denoted with $\langle S_{yx} \rangle_m$. The average measurement takes a time mT , plus computing time. Using (2)-(3), and omitting ‘ f ,’ we get

$$\langle S_{yx} \rangle_m = \frac{1}{mT} \sum_{i=1}^m (B_i A_i^* + (B_i C_i^*) + (C_i A_i^*) + (C_i C_i^*)) \quad (5)$$

Notice that $B_i A_i^*$, $B_i C_i^*$, and $C_i A_i^*$ are in general complex, while $C_i C_i^*$ is always real. The random signals $a(t)$, $b(t)$ and $c(t)$ are statistically independent because they originate from fully separate circuits.

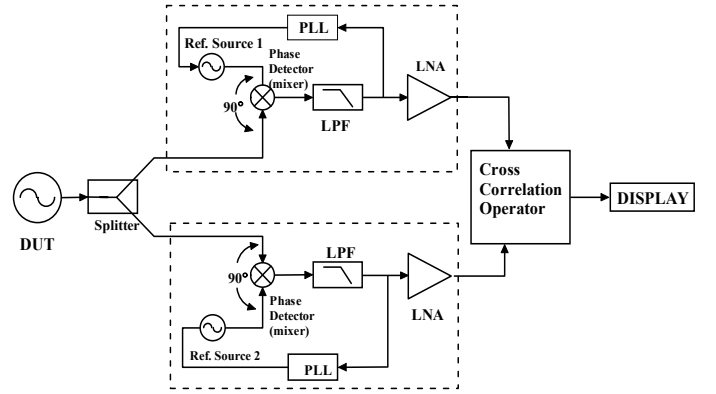


Fig. 5: A typical diagram of 2-channel cross-correlation technique

Also, and for the same reason, their Fourier transforms are statistically independent. As a consequence, the background noise ($B_i A_i^*$, $B_i C_i^*$, and $C_i A_i^*$ terms) is rejected proportionally to $\frac{1}{\sqrt{m}}$, and for large m the average $\langle S_{yx} \rangle_m$ converges to the DUT noise S_{cc} . From (5), the DUT noise through each channel is coherent and is therefore not affected by the cross-correlation, whereas, the internal noises generated by each channel are incoherent and diminish through the cross-correlation operation at the rate of \sqrt{M} (M = number of correlations), given by

$$[Noise]_{meas} = [Noise]_{DUT} + \frac{[Noise]_{channel1} + [Noise]_{channel2}}{\sqrt{M}} \quad (6)$$

where $[Noise]_{meas}$ is the total measured noise at the display; $[Noise]_{DUT}$ the DUT noise; $[Noise]_{channel1}$ and $[Noise]_{channel2}$ are the internal noise from channels 1 and 2, respectively; and ‘ M ’ is the number of correlations.

From (6), the 2-channel cross-correlation technique offers superior noise measurement capability but the measurement speed suffers when increasing the number of correlations. Figure (6) shows the measured phase noise plots (with and without cross-correlation) of 10 MHz crystal oscillator, cross-correlation offers 10-20 dB improvement in PN performance.

B. Cross-correlation: Uncertainty in PN Measurement

Cross-spectral analysis is a mathematical tool for extracting the power spectral density of a correlated signal from two time series in the presence of uncorrelated interfering signals. A major crux of the system described is the inherent impossibility to divide the DUT (device under test) noise from any other correlated effect. It is self-evident that vibrations or EMI (electromagnetic interference) hitting simultaneously on the two channels as depicted in Figure (5) cannot be rejected. However disturbing, experience is often useful to identify these perturbations as artifacts. Other effects are more subtle, and difficult to identify.

The cross-spectrum of two signals $x(t)$ and $y(t)$ is defined as the Fourier transform of the cross-covariance function of x and y . Introducing a disturbing signal $d(t)$ impacting on the two channels, from (2)-(3) rewrite as

$$x = a + c + \zeta_x d \leftrightarrow X = A + C + \zeta_x D \quad (7)$$

$$y = b + c + \zeta_y d \leftrightarrow Y = B + C + \zeta_y D \quad (8)$$

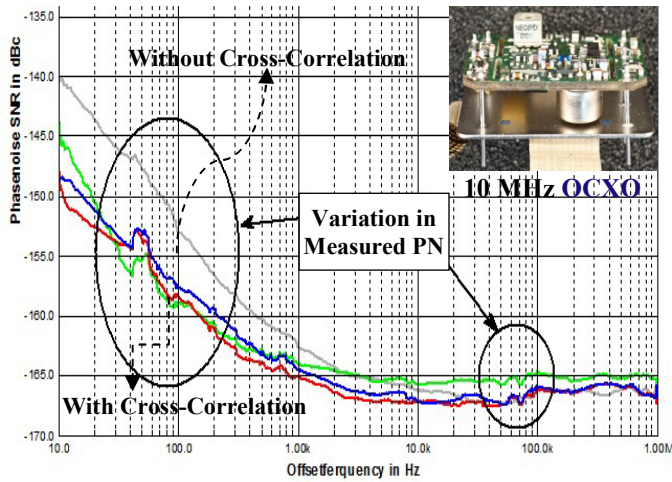


Fig. 6: Measured phase noise plots of 10 MHz OCXO circuit with/without cross-correlation (1000 correlation)

where ζ_x and ζ_y are the coefficients which describe the impact of d on the phase-to-voltage converters. Notice that ζ_x and ζ_y , and also the product $\zeta = \zeta_x \zeta_y$, can be either positive or negative. This is the case, for example, of amplitude noise, spurs, and harmonics. For the purposes of this article, rigorous measurement conducted in Faraday cage for the theoretical validation and assumption (d is statistically independent of a , b and c). This approximation has the virtue of giving physical insight on the experimental errors with very simple formalism. Having said, after averaging on a large m , the cross PSD converges to

$$S_{yx} = S_{cc} + \zeta S_{dd} \quad (9)$$

The case of $\zeta > 0$ comes with no surprise, as the experimentalist is familiar to instruments which contribute their own background noise. In the early time, the struggle for better instruments was driven by the idea that a mixer can be operated in a “sweet point” close to the quadrature, where the sensitivity to AM noise nulls. Oppositely, $\zeta < 0$ means that the instrument systematically *under-estimates the DUT noise*, as a result of the disturbing signal d . In some extreme cases S_{yx} can collapse to zero, or even be negative, which is impossible for the DUT noise. This will be unnoticed in virtually all practical cases, where the displayed quantity is $[\mathcal{L}(f)]_{dB} = 10 \cdot \log_{10}(1/2 \cdot |S_{yx}(f)|)$. Multiple disturbing signals $d_1, d_2, d_3, \dots, d_n$ may show up as bumps or dips. Even worse, if $C(f)$ and $D(f)$ have the same shape or slope versus frequency, entire octaves or decades of spectrum can be hideously under-reported, and yet looking like perfectly smooth regions in the polynomial law which describes $\mathcal{L}(f)$. Therefore, the detection of the desired signal using cross-spectral techniques collapses partially or entirely in presence of the second uncorrelated interfering signal.

III. VALIDATION EXAMPLE: 2.4 GHz SAW OSCILLATOR

Advances in time and frequency measurement have closely paralleled technological progress. High quality factor resonators (quartz crystal, MEMS, NEMS, surface acoustic wave, Bulk acoustic wave, ceramic/Dielectric resonator, and Whisper Glary mode resonator) operate at the highest possible signal to noise ratio in order to minimize the phase noise [14].

The high quality factor resonator provides the frequency-determining module; the electronic feedback system injects the energy needed to sustain the oscillation without much disturbing the resonator frequency. The sustained oscillation state forms a limit cycle in the phase space of dynamical variables of the system. A limit cycle in a deterministic system is periodic with frequency precision; divergence from this state caused due to inherent noise from thermal, electronic, vibrational and other sources [15]. In general, the oscillator phase noise will result from the combination of many different noise sources, perhaps with different spectra, leading to complicated frequency dependences for the total noise.

By varying the drive-level and optimizing the resonator nonlinearity using tuning to special operating points can improve the noise performance. Two types of noise acting directly on the resonator are expected. Firstly, thermomechanical noise for a mechanical resonator and Johnson noise for an electronic resonator. The spectrum is usually white and the noise intensity is proportional to the temperature and the dissipation coefficient. There may also be additive noise associated with the nonlinear dissipation. The second type of noise is a parameter fluctuation. The spectra of these noises may be white, white filtered by a response of the device, e.g. thermal fluctuations will be quenched above a time scale determined by thermal contact to the environment.

A. Resonator Operation in Nonlinearity Regime

The conventional approach is to drive resonator within its linear regime, which results in oscillator phase noise being inversely proportional to the oscillator carrier power. However, there is a demand for reduction in the oscillator size and power without compromising phase noise performance. When resonator is driven into its nonlinear regime, oscillation frequency becomes dependent on the amplitude of oscillation. In addition to this, with the reduction in size, their dynamic range also diminishes because nonlinear effects manifest at lower amplitudes [14].

The solution to above problems rely on the local elimination of frequency to energy dependence, evasion of amplifier noise, use of either parametric feedback, non-degenerate parametric drive, or coupling to internal resonances; however these approach are not cost-effective and offers unified solution [14]. The novel approach is to use the nonlinear behavior of the resonator to reduce the phase noise, exploiting the phase space geometry of the noise forces and the phase sensitivity of the resonator. Recent publication shows the possibility of improved phase noise performance of high q-factor resonator under nonlinear regime, where the phase noise performance is improved beyond the limitations of the linear regime. There is a possibility of existence of a special region in the parameter space, above the nonlinear threshold where the dominant contributions to the phase noise are suppressed [14]. By varying phase and feedback signals of the feedback oscillator, full exploration of the input parameter space can be obtained. The conventional phenomenological understanding is questionable, which assumes that resonator-operating regime beyond the threshold of nonlinearity necessarily degrades phase noise. The recent research reported in [14], using piezoelectric NEMS doubly clamped beam

resonator made from an aluminum nitride (AlN) and molybdenum (Mo) multilayer, operating in nonlinear region where the signal level can be increased to large values without the conventionally expected performance phase noise degradation; the improvement in phase noise performance is experimentally verified. It is therefore possible to overcome fundamental limitations of oscillator performance due to thermodynamic noise. As is known for nonlinear resonators, when the driving force is sufficiently large, the system of resonator networks can bifurcate into three possible solutions at a given drive frequency; two of these are stable, and one is unstable [16]. We report to results for the oscillator phase noise, focusing in particular on special operating points of the oscillator where the detrimental effects of the resonator noise are reduced by incorporating dynamically tuned conduction angle feedback circuitry. Figure (7) shows the typical schematic and layout of ultra low phase noise 2.4 GHz SAW oscillator circuit, where SAW resonator driven into nonlinear regime window. The reduction in phase noise is achieved by using the feedback phase to tune the oscillator to operating points where the sensitivity to particular noise sources are reduced and choosing a feedback level and phase so that the resonator is driven where the amplitude-frequency and phase-frequency curves of the driven resonator become non-monotonic. The phase noise plots shown in Figure (8) is best performance (-150 dBc/Hz @ 10 kHz offset) reported to date for this class technology.

B. Collapse of Cross-Correlation Engine: Remedy !

The cross-correlation PN measurement technique was applied to isolate any form of injection locking or inadvertent non-linearity but inherent flaw of phase inversion gave erroneous result. Figure (8) shows the misleading plot for 2.4 GHz SAW oscillator, an optimistic value of -202dBc/Hz at 1.2 MHz off the carrier and 15 dB inferior at 6 MHz offset depending upon +ve/-ve phase inversion respectively.

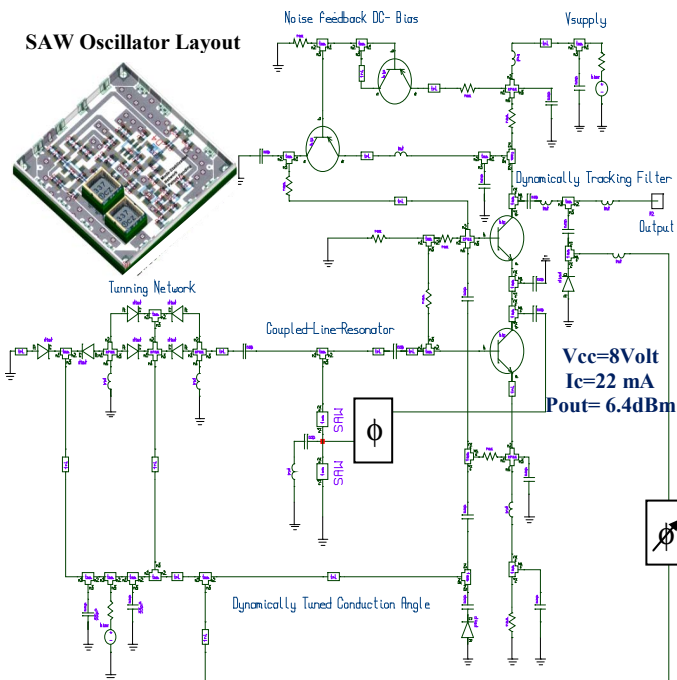


Fig. 7: A typical schematic and layout of 2.4 GHz SAW VCO

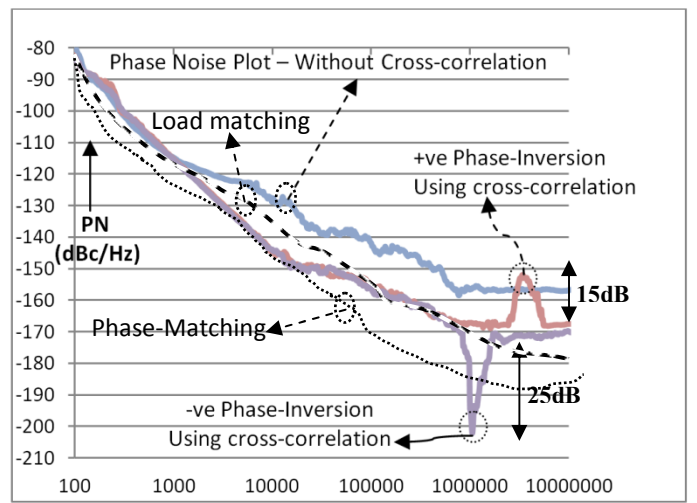


Fig. 8: Measured phase noise plots of 2.4GHz SAW oscillator circuit

We witness the variation in PN measurement due to harmonics, load and phase mismatch, and cable length (delay). These variations can be minimized by incorporating tune phase-tuned filter and impedance level at output so that impact of +ve/-ve phase inversion can be reduced significantly.

IV. CONCLUSION

The reported paper presents low phase noise 2.4 GHz SAW oscillator circuit, demonstrates stable signal source for the applications in clock and high frequency sources.

REFERENCES

- [1] D. B. Leeson, "A Simple Model of Feedback Oscillator Noise Spectrum", *IEEE Proc.* Vol. 54, pp. 329-332, 1966
- [2] T. H. Lee, A. Hajimiri, "Oscillator phase-noise: a tutorial," *IEEE J. Solid-State Circuits*, vol. 35, no. 3, pp. 326-336, March 2000.
- [3] A. Hajimiri and T. H. Lee, "A general theory of phase noise in electrical oscillators," *IEEE JSSC*, vol. 33, no. 2, pp. 179-194, Feb. 1998
- [4] Kaertner F X, "Analysis of White and 1/f Noise in Oscillators", *Int Journal of Circuit Theory and Application*, 18:485-519, 1990
- [5] Demir A., "Phase Noise and Timing Jitter in Oscillators with Colored-Noise Sources", *IEEE Trans. on CS-I*, 49(12):1782-1791, Dec 2002.
- [6] A. Demir, A. Mehrotra, and J. Roychowdhury, "Phase noise in oscillators: a unifying theory and numerical methods for characterization," *IEEE Trans. Circuits Syst. I*, vol. 47, no. 5, pp. 655 – 674, May 2000.
- [7] William Loh et al, " Unified Theory of Oscillator Phase noise I: White Noise", *IEEE Trans. on MTT*, vol. 61, No.
- [8] S. Sancho et al, "Analysis of near-carrier phase-noise spectrum in free-running oscillators in the presence of White and colored noise sources". *IEEE Trans. MTT*, Vol. 58, No. 3, March 2010, pp. 587-601.
- [9] Guide to the Expression of Uncertainty in Measurement, Fundamental Reference Document, <http://www.bipm.org/en/publications/guides/gum.html>.
- [10] P. Salzenstein and E. Pavlyuchenko, "Uncertainty Calculation for Phase Noise Optoelectronic Metrology", *PERS Proc.* pp.1099-1102, Aug 2012
- [11] E. Rubiola and R. Boudot, "The effect of AM noise on correlation phase-noise measurements," *IEEE UFFC*, vol. 54, pp. 926–932, May 2007.
- [12] C. Nelson, A. Hati, D. A. Howe, "A collapse of the cross-spectral function in phase noise metrology", *RSI* 85, 024705 (2014)
- [13] John Vig et al, "IEEE Standard Definitions of Physical Quantities for Fundamental Frequency and Time Metrology Random Instabilities," *IEEE Standard 1139-2008*, ISBN 978-0-7381-6855-5.
- [14] Villanueva et al, "Surpassing Fundamental Limits of Oscillators Using Nonlinear Resonators", *Phys Rev Lett*. 2013 April 26; 110(17): 177208
- [15] E. Kenig et al, "Optimal operating points of oscillators using nonlinear resonators," *Phys. Rev. E*, vol. 86, p. 056207, Nov 2012.
- [16] R. Lifshitz, M. Cross, "Reviews of Nonlinear Dynamics and Complexity. Schuster", Vol. 1. Wiley-VCH; Weinheim: 2008. p. 1-52.